Neutron News
Publication details, including instructions for authors and subscription information:
http://www.tandfonline.com/loi/gnnw20

Use of neutron scattering techniques for Antifreeze Protein mechanistic studies

Eduardo Howard[a], Matthew P. Blakeley[b], Andres G. Salvay[ac] & Alberto Podjarny[d]

[a] Instituto de Física de Líquidos y Sistemas Biológicos (IFLYSIB), Consejo Nacional de Investigaciones Científicas y Técnicas (CONICET), La Plata, Argentina

[b] Institut Laue-Langevin (ILL), Grenoble, France

[c] Universidad Nacional de Quilmes, Bernal, Argentina

[d] Institut de Génétique et de Biologie Moléculaire et Cellulaire (IGBMC), Centre National de la Recherche Scientifique (CNRS), Institut National de la Santé et de la Recherche Médicale (INSERM), Université de Strasbourg (UdeS), Illkirch, France

Published online: 30 Oct 2014.

To cite this article: Eduardo Howard, Matthew P. Blakeley, Andres G. Salvay & Alberto Podjarny (2014) Use of neutron scattering techniques for Antifreeze Protein mechanistic studies, Neutron News, 25:4, 24-27, DOI: 10.1080/10448632.2014.955421

To link to this article: http://dx.doi.org/10.1080/10448632.2014.955421

Use of neutron scattering techniques for antifreeze protein mechanistic studies

Eduardo Howard[1], Matthew P. Blakeley[2], Andres G. Salvay[1,3], Alberto Podjarny[4]
[1]Instituto de Física de Líquidos y Sistemas Biológicos (IFLYSIB), Consejo Nacional de Investigaciones Científicas y Técnicas (CONICET), La Plata, Argentina
[2]Institut Laue-Langevin (ILL), Grenoble, France
[3]Universidad Nacional de Quilmes, Bernal, Argentina
[4]Institut de Génétique et de Biologie Moléculaire et Cellulaire (IGBMC), Centre National de la Recherche Scientifique (CNRS), Institut National de la Santé et de la Recherche Médicale (INSERM), Université de Strasbourg (UdeS), Illkirch, France

Background

Antifreeze proteins (AFP) have evolved in organisms living in sub-zero temperatures to avoid freezing of internal fluids. They bind to ice nuclei lowering the freezing point and inhibiting recrystallization [1]. Even though this protein has been thoroughly studied, including several structures determined by X-ray crystallography, the exact mechanism of binding of ice to the largely hydrophobic Ice Binding Surface (IBS), (i.e. the region of the protein involved in the ice recognition) has remained unclear. In particular, the study of the hydration layers around the protein using X-ray crystallography did not provide a model of the IBS-ice interface.

Here we highlight the contribution of neutron scattering techniques to compare the single-crystal structure of type-III AFP with that in solution (using SANS), and to identify the hydration layers by NPC (Neutron Protein Crystallography), especially those slightly disordered, based on the special property of the strong scattering signal of deuterium atoms. As shown below, the study of the hydration layers by NPC led to a model of the IBS-ice interface.

The crystallographic study was made possible due to the availability of perdeuterated samples, which improves the signal-to-noise ratio of the diffraction data allowing one to measure radically smaller crystals than those usually used for NPC [2].

Small angle neutron scattering experiments

In order to determine the low-resolution structure in solution and the association state of type-III AFP, SANS experiments were carried out at 6 °C on the small angle neutron diffractometer D22 at the Institut Laue-Langevin (ILL, Grenoble, France). Three samples of type-III AFP at 21.6, 16.2 and 10.8 mg ml^{-1} were prepared by dissolving the lyophilized protein in pure D_2O. The transmissions of all samples were determined in the same detector/collimator configuration using 200 second exposure times.

The raw data were reduced with a standard ILL software package [3] into scattered intensities $I(Q)$, and the D_2O solvent signal subtracted from the sample signals. Figure 1a shows the experimental scattering curves (normalized to the highest concentration and scaled to 1) for type-III AFP at the three concentrations measured at 6 ºC, as well as the theoretical curve calculated from PDB entry 1HG7. In the concentration range explored, the experimental scattering curves are in excellent agreement with the theoretical curve corresponding to 1HG7 over the entire angular range. From these data, there is no evidence for any higher oligomeric states. The experimental radii of gyration (Figure 1b), 10.40 ± 0.03, 10.33 ± 0.03 and 10.28 ± 0.03 Å (type-III AFP at 21.6, 16.2 and 10.8 mg ml^{-1}) are in excellent agreement with that from the 1HG7 structure (10.2 Å). Minor differences may be due to effects of hydration shell water. In addition, we calculated a pair distance distribution function $p(r)$ from the experimental data and for the monomeric 1HG7 (Figure 1c). Both display a slightly asymmetric Gaussian shape indicative of a compact particle deviating slightly from a sphere. An *ab initio* low-resolution model was constructed from the experimental neutron scattering data and compared to the single-crystal structure using a normalized spatial discrepancy criterion (NSD). Figure 1d shows the superposition of the low-resolution model of type-III AFP and 1HG7. They are very simi-

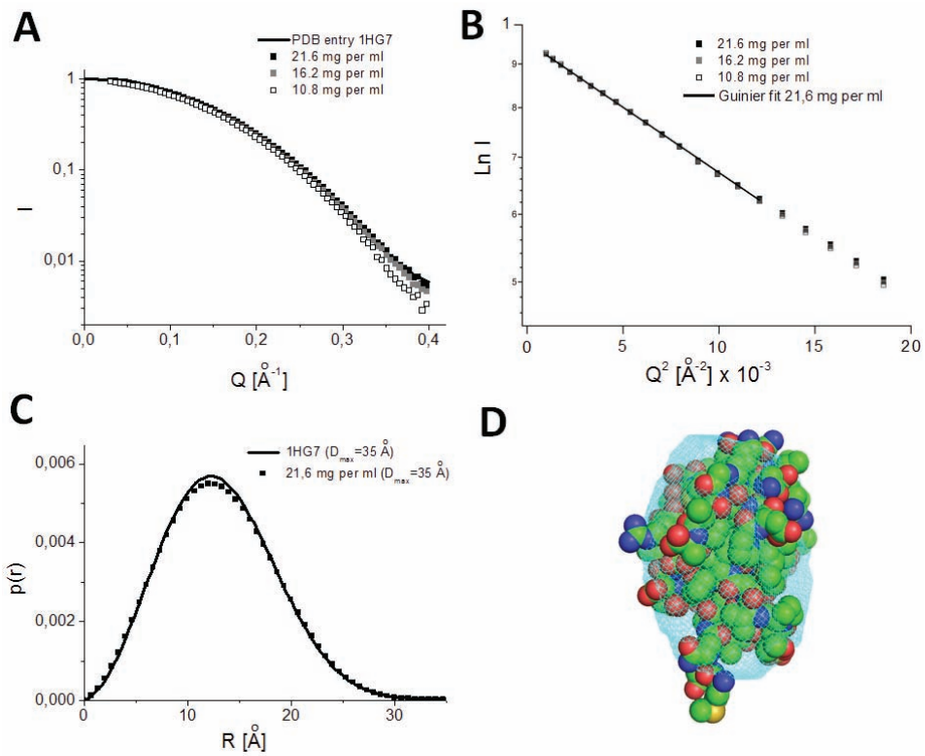

Figure 1. Small angle neutron scattering of type-III AFP at 6 °C. (a) Experimental neutron scattering curves from type-III AFP in D_2O and the theoretical curve from PDB entry 1HG7; (b) Guinier plots of the same experimental data; (c) *p*(*r*) of experimental data and back-calculated from PDB 1HG7, Dmax designs the maximum extension in real space of the particles. (d) Superposition of the low-resolution structure from experimental data and the high-resolution X-ray structure (PDB 1HG7).

lar, as reflected by a low normalized spatial discrepancy criterion NSD of 0.74 (values <1.0 indicate similarity). We therefore conclude that type-III AFP is monomeric in solution and that there are no large structural differences between the crystal structure and the structure in solution [4].

X-ray + neutron crystallographic studies

Methods

A synthetic gene of the type-III AFP [5] was overexpressed in *Escherichia coli* BL21(DE3). The perdeuterated protein was produced at the ILL Life Sciences group Deuteration Lab facility in Grenoble, France [6], where more than 99% of the 418 non-exchangeable (carbon-bound) hydrogen atoms were replaced by deuterium atoms.

The crystallization of perdeuterated type-III AFP in D_2O was carried out by the sitting-drop vapor-diffusion method [6,7] adapting the particular conditions from those of protiated type-III AFP in aqueous solution. Using these conditions, orthorhombic-shaped crystals appeared after 3 weeks and grew to maximum dimensions of 0.35 × 0.55 × 0.7 mm, corresponding to a crystal volume of 0.13 mm^3.

Perdeuterated type-III AFP crystals were measured at the ESRF beam-line ID29 at room temperature, providing X-ray diffraction data to a resolution of 1.05 Å [8].

Using a crystal with a volume of 0.13 mm^3, neutron quasi-Laue diffraction data were collected at 293 K, to 1.85 Å resolution on the LADI-III beam-line installed on cold neutron guide H142 at the Institut Laue-Langevin. The data were then scaled and merged in SCALA [9]. Data collection statistics are summarized in Table 1.

The single conformation X-ray structural model of perdeuterated type-III AFP to 1.05 Å resolution determined at room-temperature was used as the starting model for the joint X-ray + neutron refinement using the PHENIX program (version 1.6.2) [10]. D_2O molecules were added to the model according to positive nuclear

Table 1. Neutron quasi-Laue diffraction data collection statistics for the perdeuterated type-III AFP crystal with volume of 0.13 mm^3.

Neutron source, guide, instrument	Institut Laue-Langevin, cold neutron guide H142, LADI-III
Wavelength (Å)	3.18 – 4.22
No. of images	82
Setting spacing (°)	5, 7
Average exposure time (h)	6.15
Space group	$P2_12_12_1$
Unit-cell parameters	a = 32.7 Å, b = 39.1 Å, c = 46.5 Å, α = 90°, β = 90°, γ = 90°
Resolution range (Å)	32.74 – 1.85 (1.95 – 1.85)
No. of observations	71182 (3133)
No. of unique reflections	4803 (544)
Completeness (%)	89.3 (71.4)
R_{merge}	0.140 (0.195)
Mean $I/\sigma(I)$	17.5 (5.5)
Multiplicity	14.8 (5.8)

Values in parentheses are for the highest resolution shell.

density in σ_A-weighted $F_o - F_c$ maps, with manual adjustment of all D_2O molecules completed using both σ_A-weighted $2F_o - F_c$ and $F_o - F_c$ nuclear scattering density maps. A total of 73 solvent molecules were included in the final round of refinement; 64 of these could be modeled as full D_2O molecules, with another 9 exhibiting spherical nuclear scattering density and hence were modeled as O-only. The neutron R_{factor} and R_{free} values for the final model were 16.2% and 21.6%, respectively, while the X-ray R_{factor} and R_{free} values were 15.7% and 18.2%, respectively.

Results

The joint X + N refinement resulted in a model giving a very detailed description of the type-III AFP structure, including the positions of all deuterium atoms of both the protein and ordered water molecules.

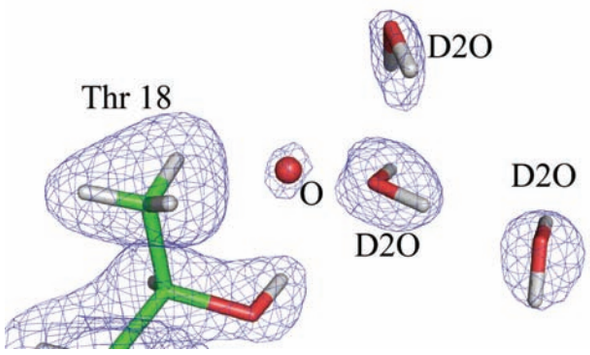

Figure 2. View of the tetrahedral water cluster bound to Thr-18 at the IBS (σ_A-weighted $2F_o - F_c$ nuclear scattering density map [contour level = 1 r.m.s.] for the tetrahedral water cluster).

The structure obtained was essentially the same as the previously published type-III AFPs. However, the joint X+N refinement led to a more complete description of the hydration layers, including both ordered (64 D_2O molecules) and slightly disordered waters (9 O-only), which are difficult to observe using X-ray diffraction data alone. The disordered water molecules do not contribute to high-resolution diffraction, and therefore this problem is not overcome by obtaining very high-resolution X-ray data.

From analysis of the nuclear scattering density maps for the solvent structure, we were able to identify a cluster of four water molecules bound to Thr-18 at the IBS with tetrahedral geometry (Figure 2). This tetrahedral water cluster was then used to fit a primary prismatic plane of ice to the protein, through a least-squares superposition using the CCP4 program LSQKAB [11]. Three waters of the tetrahedral cluster were then expanded to a six-membered water ring, which is the basic building block of the hexagonal ice structure. When doing this expansion, there are two possibilities for the water ring conformation, boat or chair. The boat conformation clearly placed the primary prismatic face roughly parallel to the orientation of the IBS plane and therefore was chosen as the most plausible orientation (Figure 3a).

From inspection of the AFP-ice interaction it was clearly observed that the hydrophobic patches (such as the methyl groups of Thr-18, Val-20, Met-21) at the IBS face the holes in the middle of the ice water rings (Figure 3b). This is in agreement with the NMR observation [12] that these hydrophobic residues make strong van der Waals interactions with ice, requiring a large interaction surface that can be provided by burying these residues in

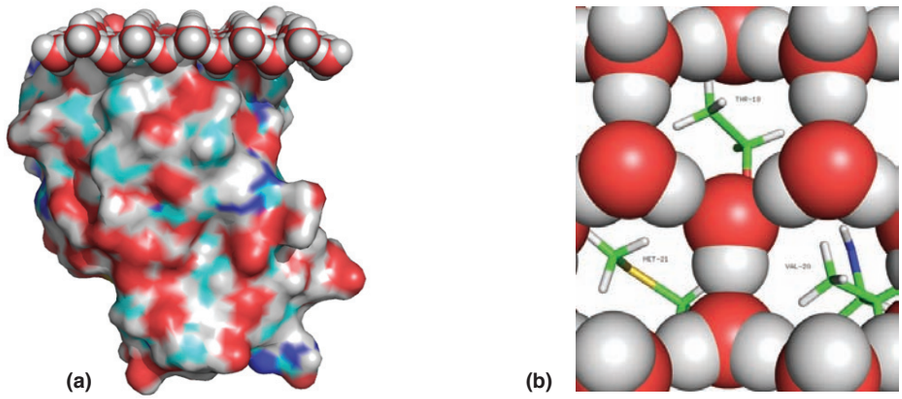

Figure 3. (a) Type-III AFP bound to a primary prismatic ice face through the IBS. The ice model is built by expansion of the experimentally determined positions of the tetrahedral water cluster. (b) Close-up of the AFP-ice interface showing the methyl groups of the hydrophobic residues Thr-18, Val-20 and Met-21, which are placed facing the holes in the ice crystal structure.

the water rings. The ice waters resulting from this model show clear hydrogen-bond interactions with the polar IBS residues.

Conclusions

Using neutron scattering techniques we have contributed to the understanding of two of the main questions in the mechanism of interaction between type-III AFP and ice.

We have proved that the type-III AFP is highly soluble and does not aggregate even at high concentrations [4], so in solution it is surrounded by liquid water.

In addition, we have observed a tetrahedral water cluster at the IBS, which has been reliably determined by the joint X + N structure determination at room temperature [8]. This cluster was used to fit a primary prismatic plane of ice. The IBS specifically recognizes local structural features present in ice but not in liquid water. Clear examples of such unique features are the holes at the centre of the water rings of ice.

We propose that the IBS of type-III AFP uses these holes to distinguish between ice and liquid water. Cold water has a short-range order similar to ice, but (contrary to ice) the holes in the middle of the six-membered water rings can be filled.

As shown above, the strong neutron diffraction signal of deuterium atoms (and therefore of water molecules) allows to reliably identify hydration features in proteins, even those that are slightly disordered. We have also shown that methodological developments, such as perdeuteration, overcome the previous limitations of NPC, such as the need for very large (>1 mm^3) crystals. The newly available spallation neutron sources combined with the methodological developments [13] should further enhance the power of NPC and enable it to be applied to many important biological questions.

References

1. S. Venketesh and C. Dayananda, *Crit. Rev. Biotechnol.* **28**, 57–82 (2008).
2. M. P. Blakeley, S. C Teixeira, I. Petit-Haertlein, I. Hazemann, A. Mitschler, M. Haertlein, E. Howard, A. D. Podjarny, *Acta Cryst.* D**66**, 1198–205 (2010).
3. R. E. Gosh, S. U. Egelhaaf, A. R. Rennie, Institute Laue Langevin internal report ILL06GH05T (2006).
4. A. G. Salvay, F. Gabel, B. Pucci, J. Santos, E. I. Howard, C. Ebel, *Biophys. J.* **99**, 609–618 (2010).
5. A. G. Salvay, J. Santos, E. I. Howard, *J. Biol. Phys.* **33**, 389–398 (2007).
6. I. Petit-Haertlein, M. P. Blakeley, E. Howard, I. Hazemann, A. Mitschler, M. Haertlein, A. D. Podjarny, *Acta Cryst.* **F65**, 406–409 (2009).
7. I. Petit-Haertlein, M. P. Blakeley, E. Howard, I. Hazemann, A. Mitschler, A. D. Podjarny, M. Haertlein, *Acta Cryst.* F**66**, 665–669 (2010).
8. E. I. Howard, M. P. Blakeley, M. Haertlein, I. Petit-Haertlein, A. Mitschler, S. J. Fisher, A. Cousido-Siah, A. G. Salvay, A. Popov, C. Muller-Dieckmann, T. Petrova, A. D. Podjarny, *J. Mol. Recognit.* **24**, 724–732 (2011).
9. P. Evans. *Acta Cryst.* D**62**, 72–82 (2006).
10. P. V. Afonine, M. Mustyakimov, R. W. Grosse-Kunstleve, N. W. Moriarty, P. Langan, P. D. Adams, *Acta Cryst.* **D66**, 1153–1163 (2010).
11. W. Kabsch, *Acta. Cryst.* **A32**, 922–923 (1976).
12. A. B. Siemer and A. E. McDermott, *J. Am. Chem. Soc.* **130**, 17394–17399 (2008).
13. M. P. Blakeley, P. Langan, N. Niimura, A. D. Podjarny, *Curr. Opin. Struct. Biol.* **18**, 1–8 (2008).